[8]Chen, C.-H., "Flutter and Time Response Analyses of Three Degrees of Freedom Airfoils in Transonic Flow," Ph.D. Dissertation, School of Aeronautics and Astronautics, Purdue Univ., Lafayette, IN, Aug. 1981.

[9]Fung, Y. C., *An Introduction to the Theory of Aeroelasticity*, Dover, New York, 1993, pp. 224, 238.

Flow Complexities of Slender Wing Rock

Lars E. Ericsson*
Mountain View, California 94040

Introduction

MILITARY design trends toward the use of unmanned, finless aircraft[1] have renewed interest in the unsteady aerodynamics of slender wing rock. One important aspect of the problem of wing rock control is the potential impact of typical configurational details on delta-wing aircraft, such as the presence of a centerbody. Early experimental results for a sharp-edged 80-deg delta wing indicated that breakdown of the leading-edge vortices played a role[2,3] (Fig. 1). It could be shown that rather than being the cause of the wing rock problem, the breakdown phenomenon limited the growth of the limit-cycle amplitude.[4] By the consideration of the effect of the roll-induced sideslip on the effective leading-edge sweep of the windward (dipping) wing-half, an upper limit for the limit-cycle amplitude could be determined.[5,6] The measured start of wing rock (Fig. 1a) is in good agreement with the prediction[7] that, for zero bearing friction, loss of roll damping should occur at $\alpha \geq 20$ deg (Fig. 2). Bearing friction caused the delay to $\alpha = 25$ deg of the loss of roll damping in the test of a pure delta-wing model[3] (Fig. 1a). It will be shown that the earlier start of wing rock for the other model[3] was caused by the presence of a centerbody or fuselage.

As even unmanned combat aircraft are likely to have a fuselage or centerbody of some kind, it is important to know that the effect of a centerbody on delta-wing aerodynamics can be large.[8] Experimental results for a 69.33-deg delta-wing–body configuration demonstrated that the centerbody promoted vortex breakdown.[9] This could be explained by the body-induced camber effect,[8,10] which according to experimental results for the effect of static camber,[11] would have promoted breakdown, in agreement with the experimental results. Figure 3 shows configurational details of the models giving the results in Fig. 1. Whereas the Langley model[2] behaves essentially as a pure, sharp-edged delta wing, the other model[3] has a centerbody. Because of its bluntness,[12] it behaves as a cylindrical centerbody,[9,10] promoting vortex breakdown, thereby causing a reduction of the maximum wing rock amplitude. The earlier loss of roll damping, before the predicted value[7] $\alpha \approx 20$ deg (Fig. 2), could also have been caused by the presence of the centerbody. By limiting the wing area, the centerbody acts to increase the effective leading-edge sweep, thereby causing earlier loss of roll damping.

The experimental results[13] in Fig. 4 show that when a pointed ogive-cylinder centerbody, similar to the one used in Ref. 9, is moved aft to start behind the wing apex, as in the case of the extensively tested 65-deg delta-wing–body configuration,[13] instead of promoting breakdown, the body delayed vortex breakdown to occur 30% or more aft of the measured position for a pure 65-deg delta-wing.[14] It is described in Ref. 5 how this is the expected result when the pointed ogive-cylinder body is moved aft, as shown in Fig. 4,

Presented as Paper 99-0141 at the 37th Aerospace Sciences Meeting, Reno, NV, 11–14 January 1999; received 15 February 1999; accepted for publication 13 April 2000.

*Consulting Engineer. Fellow AIAA.

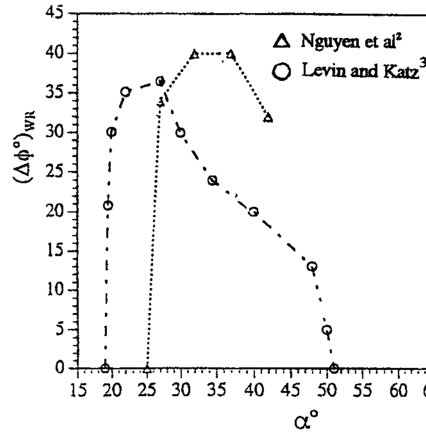

a) Measured wing rock amplitude[2,3]

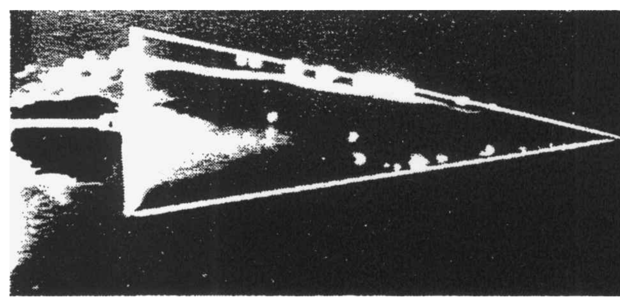

b) Flow visualization of vortex breakdown at $\sigma = 25$ deg (Ref. 3)

Fig. 1 Wing rock of 80-deg delta wing.

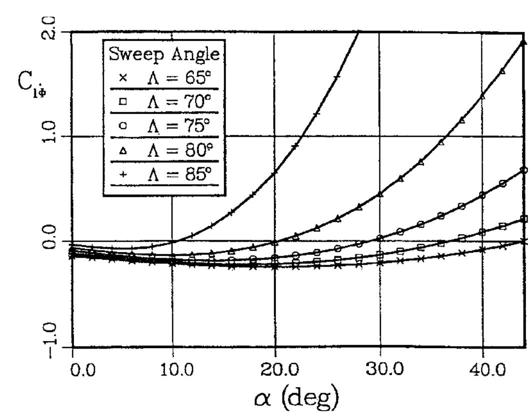

Fig. 2 Effect of leading-edge sweep on delta wing roll damping.[7]

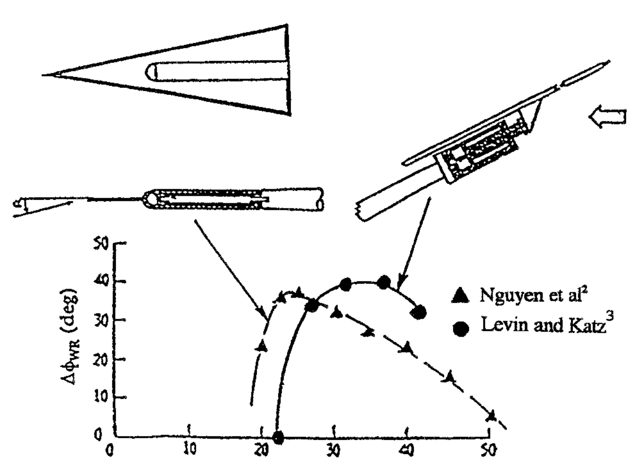

Fig. 3 Effect on wing rock results of geometric details of the test model.[2,3]

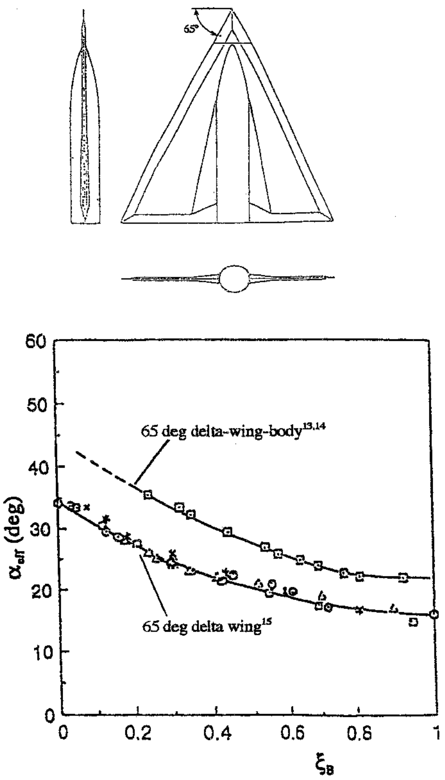

Fig. 4 Measured breakdown location on a 65-deg delta-wing–body configuration[13] compared with that on a pure delta wing.[14]

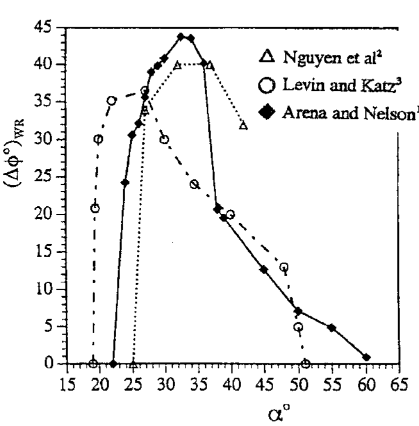

Fig. 5 Slender wing rock amplitude envelope.[2,3,15]

causing the body-induced camber effect to become of the opposite type, delaying vortex breakdown.[8]

Flow Complexities

Figure 5 shows that the experimental results obtained in tests with a close to frictionless air-bearing[15] agree well with the earlier results[2,3] (Fig. 1). The complexity arises from the following statement made in Ref. 15: "Vortex breakdown was not observed on the wing at any time up to and including 36-deg angle of attack." That appears at first to contradict the flow physics described earlier, based on the results[2,3] in Fig. 1. However, the experimental results[15,16] in Figs. 6 and 7 provide the clues needed to resolve this dilemma. The results[16] for the 80-deg delta wing in Fig. 6 for 40-deg inclination σ of the roll axis show that two widely different amplitude time histories could be measured depending on whether or not vortex breakdown was observed to occur on the wing before the start of the oscillation. Without initial breakdown forward of the trailing edge, the wing rock oscillations reached amplitudes approaching 35 deg

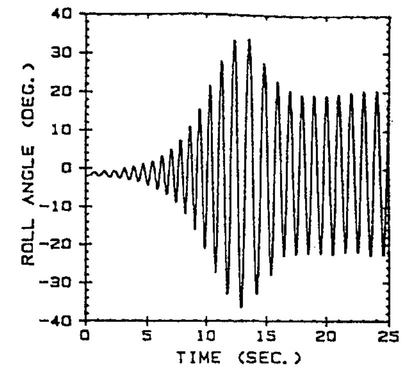

a) Without breakdown on wing

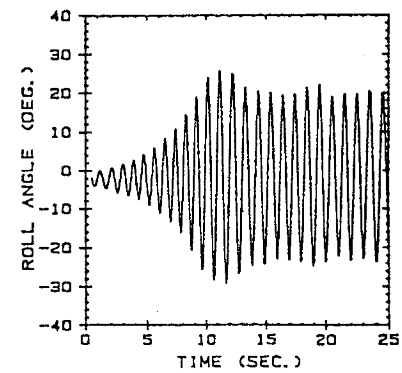

b) With initial breakdown on wing

Fig. 6 Wing rock time histories at σ = 40 deg of 80-deg delta wing.[17]

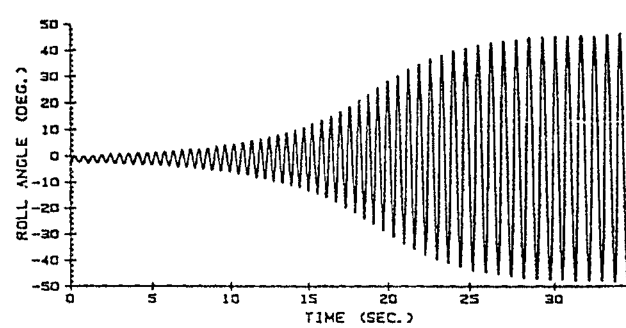

Fig. 7 Wing rock time histories at σ = 30 deg of 80-deg delta wing.[18]

before settling down to $\Delta\phi \approx 20$ deg (Fig. 6a). In the other case (Fig. 6b), where breakdown occurred on the wing from the start, only a modest overshoot to $\Delta\phi \approx 25$ deg was recorded before the amplitude reached its final 20-deg value. These wing rock characteristics are very different from those observed at $\sigma = 30$ deg (Ref. 17 and Fig. 7), which are of the same type as those observed in earlier tests.[2,3]

The results in Figs. 6 and 7 indicate the likely presence of σ hysteresis, which could be expected according to Lowson's results for an 80-deg delta wing (see Ref. 18). Based on these observations one is inclined to conclude that the reason that the Notre Dame wing rock results[16] approached the predicted maximum possible amplitude,[5,6] whereas the earlier test results[2,3] did not (Fig. 5), was that vortex breakdown behaved somewhat in the manner assumed in reaching the maximum amplitude limit.[5,6] That is, at a constant σ, vortex breakdown is initially hung up behind the trailing edge until (at $\phi = 0$) flow unsteadiness[18] or a change to $\phi \neq 0$ causes it to jump forward of the trailing edge. This implies that on a maneuvering delta-wing aircraft the experienced wing rock depends strongly on the preceding maneuver time history.

Because vortex breakdown is absent below $\alpha = 36$ deg in the Notre Dame test[15] (Fig. 5) another flow mechanism limits the amplitude growth in that alpha region. One such flow mechanism is the roll-rate-induced camber effect discussed extensively in the analysis of the 65-deg delta-wing–body configuration (Fig. 4).[19] A direct demonstration of the roll-rate-induced camber effect, with its associated roll damping, is provided by the test results at zero angle of attack for a rolling 80-deg delta wing[20] (Fig. 8). Figure 8 shows how the vortex-induced suction peaks increase in magnitude with increasing roll rate $K = \dot{\phi} b / 2U_\infty$. The blemish in Fig. 8 is the difference between the vortex-induced loads on the two wing halves. Looking at how the load distributions change with chordwise location (Fig. 8b), one finds that the relative difference increases with increasing proximity to the trailing edge. Close scrutiny of the test setup (Fig. 9) reveals that a large, asymmetric structure, used to enclose the drive shaft, was located within two chord lengths from the trailing edge of the delta wing. It is likely to have caused early vortex breakdown on the upstroking wing half ($\eta < 0$ in Fig. 8). This is in agreement with the observed effect on trailing forebody vortices caused by a downstream support structure.[21] The decreased suction level upstream of $\xi = 0.958$ on the port, left-hand side ($\eta < 0$) compared to the opposite side ($\eta > 0$) in Fig. 8b is a result of the upstream interference from the breakdown region near the trailing edge. This interference apparently does not become of negligible magnitude until forward of the midchord, $\xi < 0.5$.

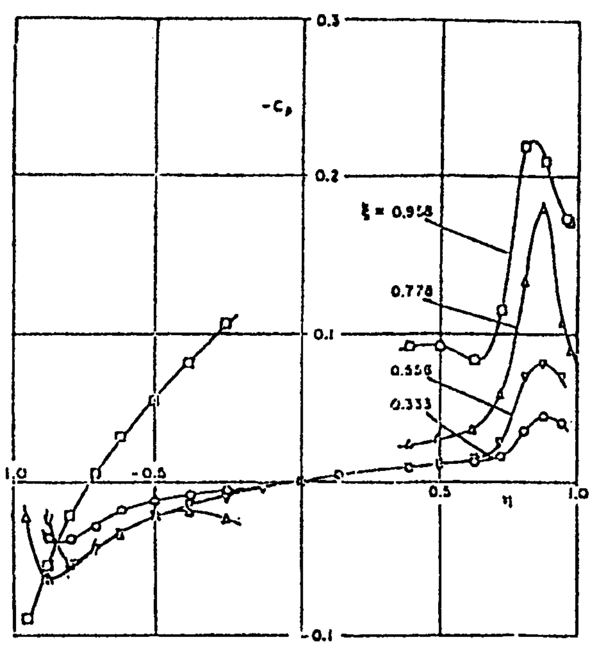

a) Effect of roll rate on the spanwise load distribution at $\xi = 0.778$

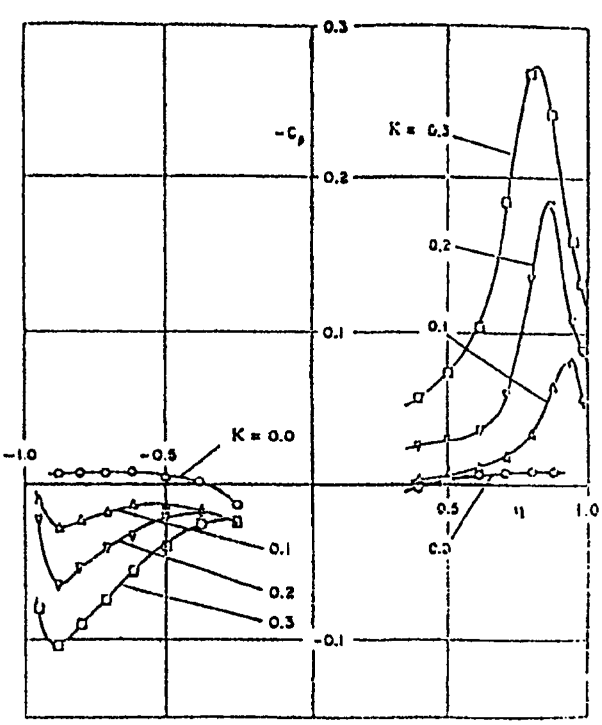

b) Effect of chordwise location on the roll-rate-induced spanwise load distribution at $K = 0.20$

Fig. 8 Roll-rate-induced roll damping moment at $\sigma = 0$ on an 80-deg delta wing.[21]

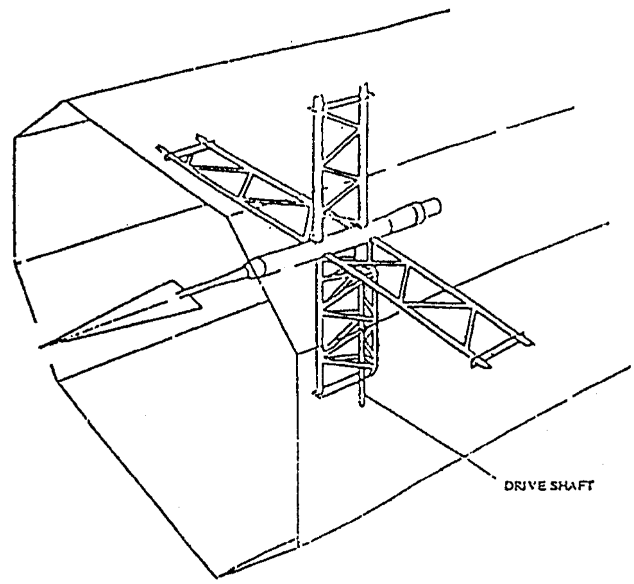

Fig. 9 Asymmetric support structure for the rolling 80-deg delta wing.[21]

Conclusions

An analysis of the existing experimental and theoretical database has revealed that the already complex flow physics of slender wing rock are complicated further by the presence of a fuselage or centerbody. It appears that in general the development of efficient means for wing rock control on delta-wing aircraft will require experimental and theoretical investigations tailored to its unique configurational details.

References

[1] Fulghum, D. A., "ARPA Explores Unmanned Combat Aircraft Designs," *Aviation Week and Space Technology*, Feb. 1996, pp. 23–25.

[2] Nguyen, L. E., Yip, L. P., and Chambers, J. R., "Self-Induced Wing Rock of Slender Delta Wings," AIAA Paper 81-1883, Aug. 1981.

[3] Levin, D., and Katz, J., "Dynamic Load Measurements with Delta Wings Undergoing Self-Induced Roll-Oscillations," *Journal of Aircraft*, Vol. 21, No. 1, 1984, pp. 193–199.

[4] Ericsson, L. E., "The Fluid Mechanics of Slender Wing Rock," *Journal of Aircraft*, Vol. 21, No. 5, 1984, pp. 322–328.

[5] Ericsson, L. E., "Analytic Prediction of the Maximum Amplitude of Slender Wing Rock," *Journal of Aircraft*, Vol. 26, No. 1, 1989, pp. 35–39.

[6] Ericsson, L. E., "Rapid Prediction of Wing Rock for Slender Delta Wing Configurations," *Journal of Aircraft*, Vol. 35, No. 6, 1998, pp. 979–981.

[7] Ericsson, L. E., and King, H. H. C., "Rapid Prediction of High-Alpha Unsteady Aerodynamics of Slender-Wing Aircraft," *Journal of Aircraft*, Vol. 29, No. 1, 1992, pp. 85–92.

[8] Ericsson, L. E., "Effect of Fuselage on Delta Wing Vortex Breakdown," *Journal of Aircraft*, Vol. 35, No. 6, 1998, pp. 898–904.

[9]Straka, W. A., and Hemsch, M. J., "Effect of Fuselage on Delta Wing Vortex Breakdown," *Journal of Aircraft*, Vol. 31, No. 4, 1994, pp. 1002–1005.

[10]Ericsson, L. E., "Comment on 'Effect of Fuselage on Delta Wing Vortex Breakdown,'" *Journal of Aircraft*, Vol. 31, No. 4, 1994, pp. 1006, 1007.

[11]Lambourne, N. C., and Bryer, D. W., "The Bursting of Leading-Edge Vortices—Some Observations and Discussion of the Phenomenon," R&M 3282, Aerodynamic Research Council, England, U.K., April 1961.

[12]Ericsson, L. E., "Further Analysis of Fuselage Effects on Delta Wing Aerodynamics," AIAA Paper 2000-0981, Jan. 2000.

[13]Hanff, E. S., and Jenkins, S. B., "Large Amplitude High-Rate Roll Experiments on a Delta and Double Delta Wing," AIAA Paper 90-0224, Jan. 1990.

[14]Lowson, M. V., and Riley, A. J., "Vortex Breakdown Control by Delta Wing Geometry," *Journal of Aircraft*, Vol. 32, No. 4, 1995, pp. 832–838.

[15]Arena, A. S., Jr., and Nelson, R. C., "Experimental Investigations on Limit Cycle Wing Rock of Slender Wings," *Journal of Aircraft*, Vol. 31, No. 5, 1994, pp. 1148–1155.

[16]Arena, A. S., Jr., and Nelson, R. C., "The Effect of Asymmetric Vortex Wake Characteristics on Slender Delta Wing Undergoing Wing Rock Motion," AIAA Paper 89-3348, Aug. 1989.

[17]Jun, Y. W., and Nelson, R. C., "Leading-Edge Vortex Dynamics on a Delta Wing Undergoing Wing Rock Motion," AIAA Paper 87-0332, Jan. 1987.

[18]Lowson, M. V., "Some Experiments with Vortex Breakdown," *Journal of the Royal Aeronautical Society*, Vol. 68, May 1964, pp. 343–346.

[19]Ericsson, L. E., and Hanff, E. S., "Further Analysis of High-Rate Rolling Experiments of a 65-Degree Delta Wing," *Journal of Aircraft*, Vol. 31, No. 6, 1994, pp. 1350–1357.

[20]Harvey, J. K., "A Study of the Flow Field Associated with a Steadily Rolling Slender Delta Wing," *Journal of the Royal Aeronautical Society*, Vol. 68, Feb. 1964, pp. 106–110.

[21]Ericsson, L. E., and Beyers, M. E., "Ground Facility Interference Effects on Slender Vehicle Unsteady Aerodynamics," *Journal of Aircraft*, Vol. 33, No. 1, 1996, pp. 117–124.

Elastomeric Damper Model and Limit Cycle Oscillation in Bearingless Helicopter Rotor Blade

G. Pohit,* C. Venkatesan,† and A. K. Mallik‡
Indian Institute of Technology, Kanpur, U.P. 208 016, India

I. Introduction

WITH the advancement in technology, development of a mechanically simple yet efficient rotor blade system has resulted in the design of a bearingless blade and hub configuration.[1] A schematic diagram of a bearingless rotor blade is shown in Fig. 1. In this rotor system (Fig. 1), the blade is attached to the hub through a flexbeam that is designed to provide the required stiffness in the flap and lag bending deformation of the blade, but that is highly flexible in torsion. Surrounding the flexbeam, there is a stiff cuff denoted as the torque tube, which is attached to the blade–flexbeam junction at the outboard end and to a pitch link at the inboard end, as shown in Fig. 1. The pitch control of the blade is achieved by rotating the torque tube through the up/down movement of the point P, which, in turn, twists the flexbeam. An elastomeric damper is placed between the torque tube and flexbeam to provide adequate lag damping. It also acts as a spacer between the torque tube and the flexbeam. Though a bearingless rotor is mechanically simple, its dynamic analysis becomes complicated due to the presence of a multiple load path and a nonlinear elastomeric damper.

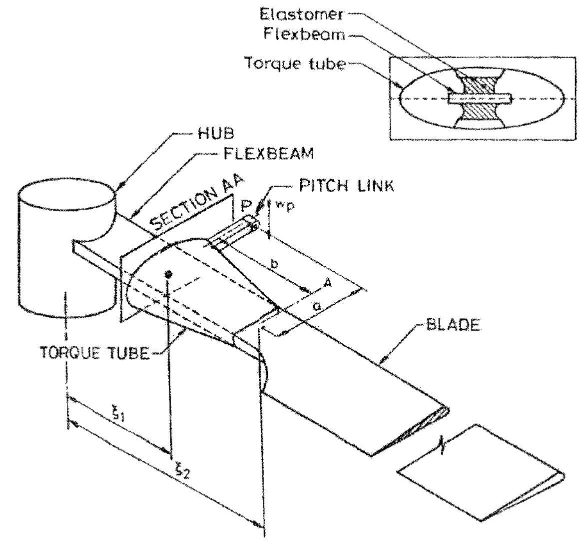

Fig. 1 Bearingless rotor blade with pitch link at the leading edge.

The nonlinear dynamic characteristics of the elastomer are usually represented by the variation of in-phase stiffness (stiffness) and quadrature stiffness (damping) as a function of amplitude. The experimental results of a single frequency bench test of different elastomeric lag dampers are available in Refs. 2–4. All of these data indicate that both the in-phase stiffness K' and the quadrature stiffness K'' decrease as the amplitude of motion increases. The variation of loss tangent or loss factor η with amplitude is also shown in Ref. 3. Loss tangent is generally defined as the ratio of K'' and K'. In a recent publication, Kunz[5] also indicated similar types of stiffness and damping characteristics of the elastomer with respect to the amplitude of motion.

There are several linear models to describe the mechanical behavior of visco-elastic materials, for example, anelastic displacement fields (ADF) have been used in Ref. 6. Smith et al.[7] extended the method of ADF to include the nonlinearities and temperature effects. The nonlinear characteristics of elastomers have been analyzed in detail in several recent publications.[8–12] Some of the recent studies have focused on the phenomenon of the limit-cycle behavior of bearingless rotor blades due to the elastomer nonlinearity. In Ref. 11, Gandhi and Chopra proposed a nonlinear viscoelastic model for the elastomer in which the damping element is linear. The model shows a rapid decrease in damping coefficient at very low amplitudes of oscillation, but its value is always positive. With this elastomeric damper, they showed a limit-cycle oscillation for an autonomous system representing the isolated lag dynamics of a blade. Ormiston et al.[13] considered an elastomer model in which the damping force was assumed to be proportional to a linear combination of different powers of velocity (powers of 0.5, 1, 2, and 3). Using this nonlinear elastomer model, they showed the presence of limit-cycle oscillation for both hingeless and bearingless rotor blade configurations. It was also pointed out that there was no limit cycle when the elastomer damping is taken as linear. The hover air-resonance analysis and wind-tunnel test by Panda and Mychalowycz[1] also indicated that nonlinearities in stiffness and damping characteristics of the elastomer seem to have a significant influence on the limit-cycle oscillations. When they used a fluidlastic damper having linear characteristics, no limit-cycle oscillation was observed.

The objective of the present Note is to analyze the relation between elastomer modeling and limit-cycle oscillation. The example problem chosen to address this is the transient response behavior of an isolated bearingless rotor blade undergoing coupled flap–lag–torsional deformation under a hovering condition. The

Received 18 July 1999; revision received 13 June 2000; accepted for publication 17 June 2000.

*Graduate Student, Department of Mechanical Engineering.
†Professor, Department of Aerospace Engineering. Senior Member AIAA.
‡Professor, Department of Mechanical Engineering.